Executive Summary

EXPERIMENTAL INVESTIGATION OF SKEWED ELASTOMERIC EXPANSION BRIDGE BEARINGS

by

Gregory D. Allen
and
Thomas M. Murray
Principal Investigator

Fears Structural Engineering Laboratory
University of Oklahoma
Norman, Oklahoma 73019

Sponsored by

Oklahoma Department of Transportation
Research and Development Division

in cooperation with the

Federal Highway Administration

Report No. FSEL/ODOT 87-01

April 1987

This publication was printed and issued by the Oklahoma Department of Transportation as authorized by V. O. Bradley, Director. 130 copies have been prepared and distributed at a cost of $168.60.

TECHNICAL REPORT STANDARD TITLE PAGE

1. REPORT NO. FHWA/OK 87(3)	2. GOVERNMENT ACCESSION NO.
3. RECIPIENT'S CATALOG NO.	
4. TITLE AND SUBTITLE Experimental Investigation of Skewed Elastomeric Expansion Bridge Bearings	5. REPORT DATE April 1987
	6. PERFORMING ORGANIZATION CODE
7. AUTHOR(S) Gregory D. Allen and Thomas M. Murray	8. PERFORMING ORGANIZATION REPORT
9. PERFORMING ORGANIZATION NAME AND ADDRESS Fears Structural Engineering Laboratory University of Oklahoma 303 E. Chesapeake St. Norman, OK 73019	10. WORK UNIT NO.
	11. CONTRACT OR GRANT NO. Agreement #34, 84-11-2
12. SPONSORING AGENCY NAME AND ADDRESS Research and Development Division Oklahoma Department of Transportation 200 NE 21st Oklahoma City, OK 73105	13. TYPE OF REPORT AND PERIOD COVERED Executive Summary Jan '85 - April '87
	14. SPONSORING AGENCY CODE

15. SUPPLEMENTARY NOTES In cooperation with

Federal Highway Administration, US Department of Transportation

16. ABSTRACT Twelve skewed elastomeric expansion bridge bearings were supplied by the Oklahoma Department of Transportation. To evaluate the performance of these skewed bearings, the following six phases of testing were conducted on each of the twelve bearings: I. Shear and compressive stiffness tests, II. Fatigue cycles representing 50 years of service with parallel bearing surfaces, III. Shear and compressive stiffness tests, IV. Shear stiffness tests with bearings at sub-freezing temperatures, V. Fatigue cycles representing 50 years of service with rotated bearing surfaces, and VI. Shear stiffness tests. Phase I formed the basis of comparison with the post-fatigue results from Phases III and VI, and the low temperature tests from Phase IV. It was found that the fatigue loading with parallel bearing surfaces had very little effect on the compressive and shear stiffnesses of the skewed bearings. Some degradation of shear stiffness was found after the fatigue loading with rotated bearing surfaces, Phase V. However, the combined degradation due to both fatigue loadings was considered insignificant.

It was found that the simple shear equation for estimating the shear stiffnesses of the twelve bearings was very conservative and no correlation was evident between predictions and the experimental results of Phase I. In general, the shear stiffness changed more rapidly than the change in bearing area as the skew angle decreased from 90° (rectangular) to 30°.

As an outgrowth of the experimental work, design expressions for determining the effective shear stiffnesses of both skewed and rectangular bearings with turned axes were developed. Excellent correlation was found between shear stiffness predictions from the proposed equations and the experimental results.

17. KEY WORDS skew, bearings, elastomeric, bridges, shear stiffness, expansion device, shear modulus	18. DISTRIBUTION STATEMENT no restrictions

19. SECURITY CLASSIF. (OF THIS REPORT) none	20. SECURITY CLASSIF. (OF THIS PAGE) None	21. NO. OF PAGES 30	22. PRICE

TABLE OF CONTENTS

LIST OF FIGURES

LIST OF TABLES

NOMENCLATURE

a = long dimension of rectangular bearing

A = plan area of undeformed bearing

A_e = effective area of bearing

b = short dimension of rectangular bearing

G = shear modulus

I = moment of inertia of the bearing plan area taken about an axis perpendicular to the girder axis

k = shear stiffness

k_c = the compressive stiffness, secant modulus defined at the design dead load levels of the elastomeric bearings

$(k_s)_\alpha$ = skewed bearing shear stiffness for any given skew angle α

$(k_t)_\alpha$ = turned bearing shear stiffness for turned angle α

L = length of skewed bearing parallel to girder axis

t_i = thickness of an internal elastomeric layer

T = Σt_i, sum of the internal elastomeric layer thicknesses

V = shear force

W = width of skewed bearing perpendicular to girder axis

α = bearing skewed or turned angle

δ_s = maximum required horizontal displacement of an elastomeric bearing

Δ_s = sum of shearing and bending displacements of laterally deformed elastomeric bearing

Executive Summary

EXPERIMENTAL INVESTIGATION OF SKEWED ELASTOMERIC EXPANSION BRIDGE BEARINGS

CHAPTER I

INTRODUCTION

1.1 Background

Expansion and contraction caused by temperature, deflection, relative support settlement, creep, etc., will produce longitudinal motion in a bridge. Elastomeric bearings allow longitudinal motion to take place and transmit forces to the abutments or piers because of shear deformations. Current AASHTO specification provisions [1] are written for elastomeric bearings that are rectangular in shape with all movement perpendicular to the centerline of the bearing.

If a bridge spans a river or a highway that is not perpendicular to it, movement other than that parallel to the centerline of the bearing may have to be accommodated. Two methods of providing for movement when abutments or piers are skewed with respect to the bridge centerline are shown in Figures 1.1 and 1.2. Figure 1.1 shows a "skewed bearing"; Figure 1.2 illustrates a "turned bearing". Proper design of skewed and turned elastomeric bearings requires a knowledge of shear stiffness or the load-shear deformation relationship, compressive stiffness or the load-compression relationship, low temperature, and effects of fatigue, and out-of-plane rotation.

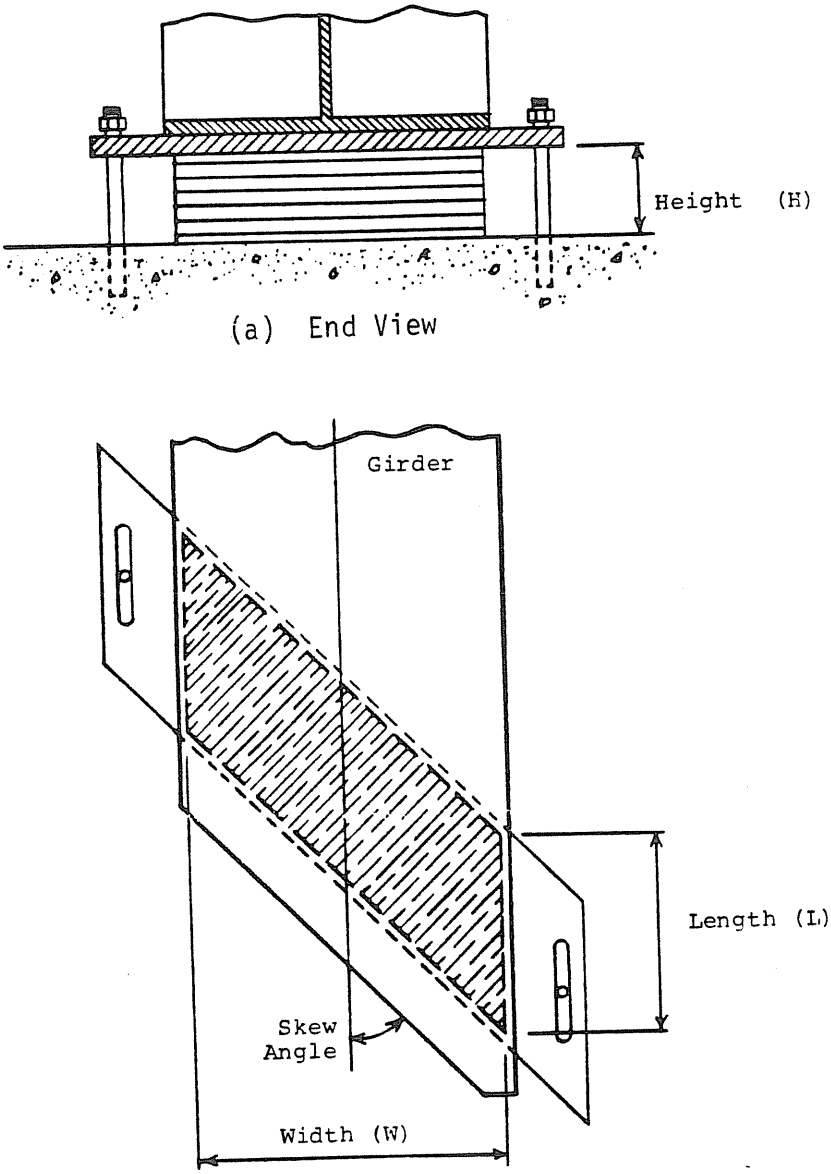

Figure 1.1 Typical Skewed Bearing

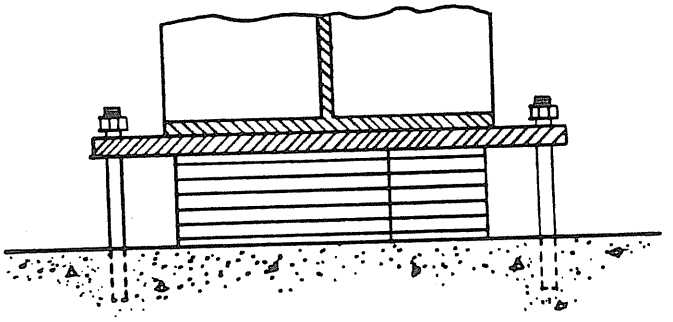

(a) End View

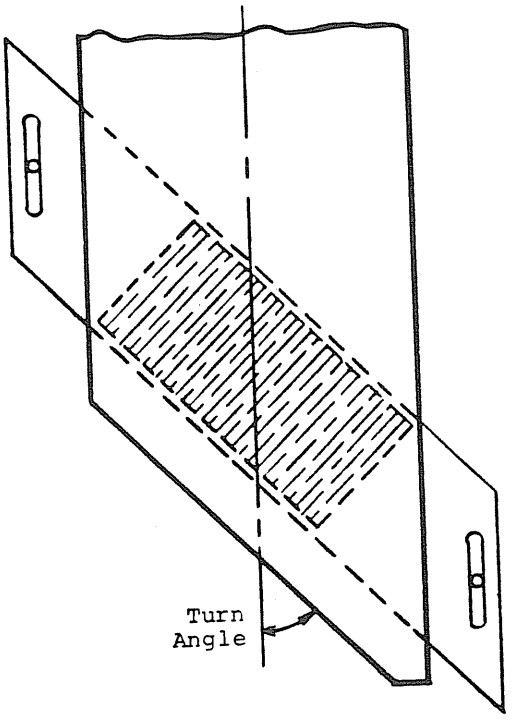

(b) Plan View

Figure 1.2 Typical Turned Bearing

1.2 Purpose of Study

The primary purpose of this study was to experimentally determine the effective shear stiffness and the behavior at low temperatures of twelve skewed elastomeric bearings. A secondary purpose was to investigate the effects of bridge girder end rotations and the performance of bearings under fatigue loading. An outgrowth of the experimental work was the development of design expressions for determining the effective shear stiffnesses of both skewed and turned bearings. Reference 2 is a complete description of the study; what follows is a brief summary.

1.3 Test Bearing Parameters

The Oklahoma Department of Transportation (ODOT) supplied twelve elastomeric bearings which consisted of a variable number of 1/2 in. thick layers of Neoprene bonded together by 14 gage steel laminates. The design parameters for the bearings were determined by ODOT and included skew angle, height, width and length as defined in Table 1.1.

The bearings were divided into three series, A, D and E, corresponding to design bearing heights of 3 7/16 in., 6 5/16 in. and 1 3/4 in., respectively. Each series included bearings having skew angles, as defined in Figure 1.1, of 90°, 60°, 45° and 30°, thus the designations A90, D60, etc. Tables 1.1 and 1.2 are summaries of the bearing geometric parameters (internal bearing details, skew angle, height, width and length) and bearing test parameters (maximum design shear displacement, area, shape factor, Neoprene hardness as measured with a Shore A Type durometer, shear modulus and design loads), respectively.

Table 1.1

Skewed Bearing Design Parameters

Bearing Pad Series	Internal Bearing Details	Skew Angle (deg)	H Height (in)	W Width (in)	L Length (in)
A	7 ply Neoprene 5 inner plies of 1/2 in. 2 cover plies of 1/4 in. 6-14 Ga. laminates	90 60 45 30	3 7/16	18	9 9 5/8 10 1/2 12
D	12 ply Neoprene 10 inner plies of 1/2 in. 2 cover plies of 1/4 in. 11-14 Ga. laminates	90 60 45 30	6 5/16	16 1/2	16 1/2 17 1/4 18 1/2 21
E	4 ply Neoprene 2 inner plies of 1/2 in. 2 cover plies of 1/4 in. 3-14 Ga. laminates	90 60 45 30	1 3/4	18	17 17 1/4 18 1/2 21

Table 1.2

Skewed Bearing Geometric and Measured Parameters

Bearing	Max. Design Displacement (in)	Area (in^2)	Shape Factor	Durometer Reading* (hardness)	Shear Modulus (psi)	Design Loading (kips)
A90 A60 A45 A30	1 1/2	162.0 173.3 189.0 216.0	6.0 5.7 5.3 4.5	55 60 57 58	105 128 111 114	RDL = 75 RLL = 40 TL = 115
D90 D60 D45 D30	2 3/4	272.3 284.6 305.3 346.5	8.3 7.9 7.3 6.4	55 62 60 59	105 128 120 117	RDL = 190 RLL = 40 TL = 265
E90 E60 E45 E30	3/4	306.0 310.5 333.0 378.0	8.7 8.2 7.6 6.6	55 61 56 58	105 124 108 114	RDL = 215 RLL = 85 TL = 300

Note: RDL = Dead Load Reaction
RLL = Live Load Reaction
TL = Total Load

*Measured

1.4 Scope of Study

To evaluate the performance of skewed elastomeric expansion bearings, the following six phases of testing were conducted on each of the twelve bearings:

I. Shear and compressive stiffness tests using previously unloaded bearings.

II. Shear-fatigue cycles representing 50 years of service with parallel top and bottom bearing surfaces.

III. Shear and compressive stiffness tests immediately following Phase II.

IV. Shear stiffness tests with bearings at sub-freezing temperatures and after the bearings had been tested in Phases II and III.

V. Additional shear-fatigue cycles representing 50 years of service with the bearing rotated such that one of the contact surfaces was at a 2% slope with respect to the other surface.

VI. Shear stiffness tests upon the completion of Phase V.

Phase I formed the basis of comparison with the post-fatigue results of Phases III and VI. The testing phases were also scheduled so that the low temperature test results of Phase IV could be compared with the results of Phase III.

CHAPTER II

TESTING DETAILS

2.1 Test Setup

In an actual bridge, the expansion and contraction of a bridge girder due to temperature changes causes a longitudinal displacement at the girder ends. This displacement is achieved through the shear deformation of the elastomeric bearing. The dead and live loads of the bridge are transferred through the girders causing the bearings to compress. Thus, a test setup was needed to allow the bearing to compress freely and to force the bearing to move to the design shear displacement as if the bearing was part of an actual bridge system.

To determine the experimental compressive behavior and the shear stiffnesses of the elastomeric bearings, a test setup which simulates an actual bridge was erected inside Fears Structural Engineering Laboratory on the laboratory reaction floor; details are shown in Figures 2.1 and 2.2. The normal force was applied with a 400,000 lb. capacity hydraulic ram and the horizontal force with a 55,000 lb. capacity closed-loop hydraulic testing system capable of cyclic loading.

2.2 Instrumentation

Instrumentation consisted of two calibrated load cells, two horizontal and four vertical displacement transducers,

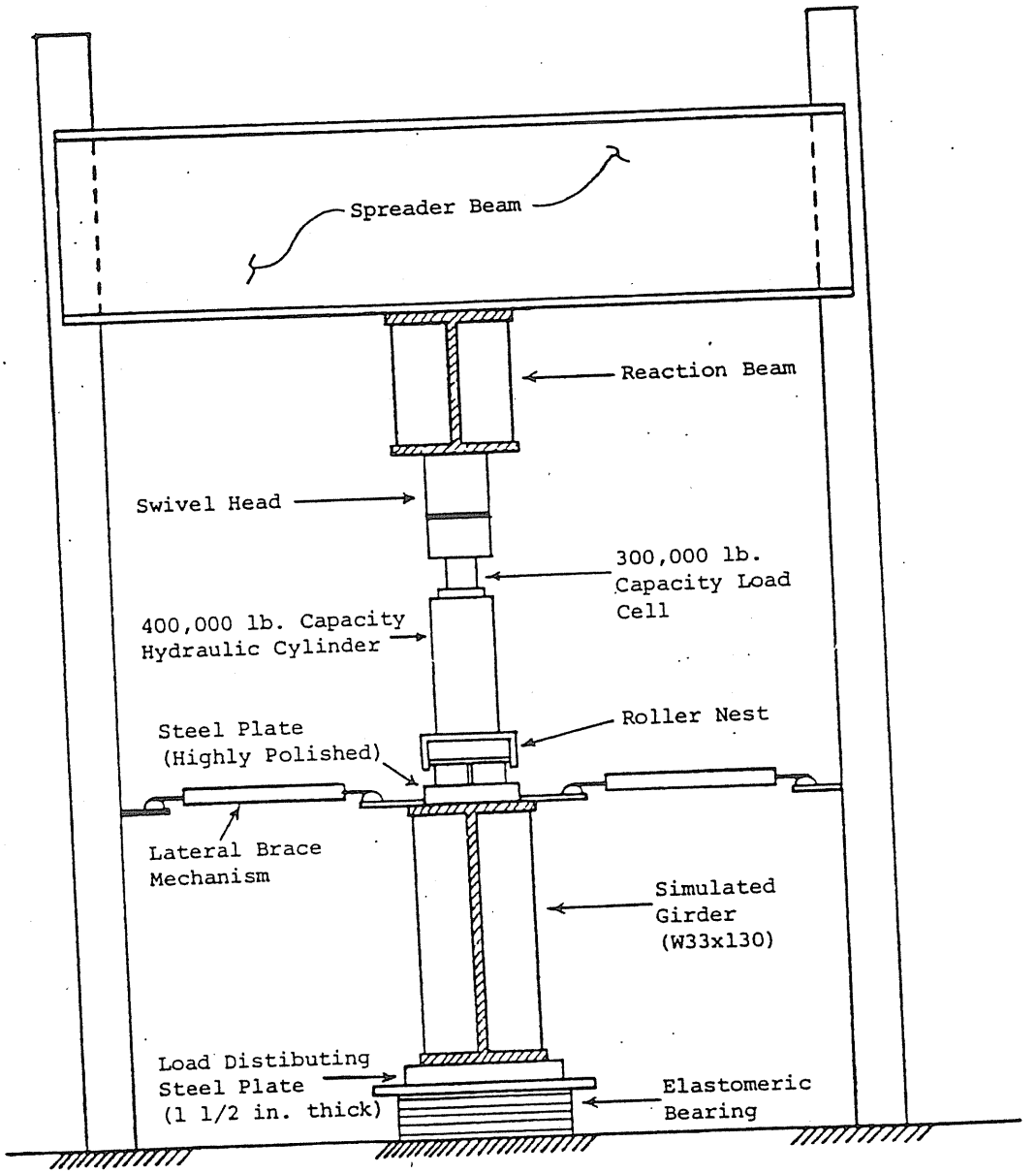

Figure 2.1 Vertical Load Chain

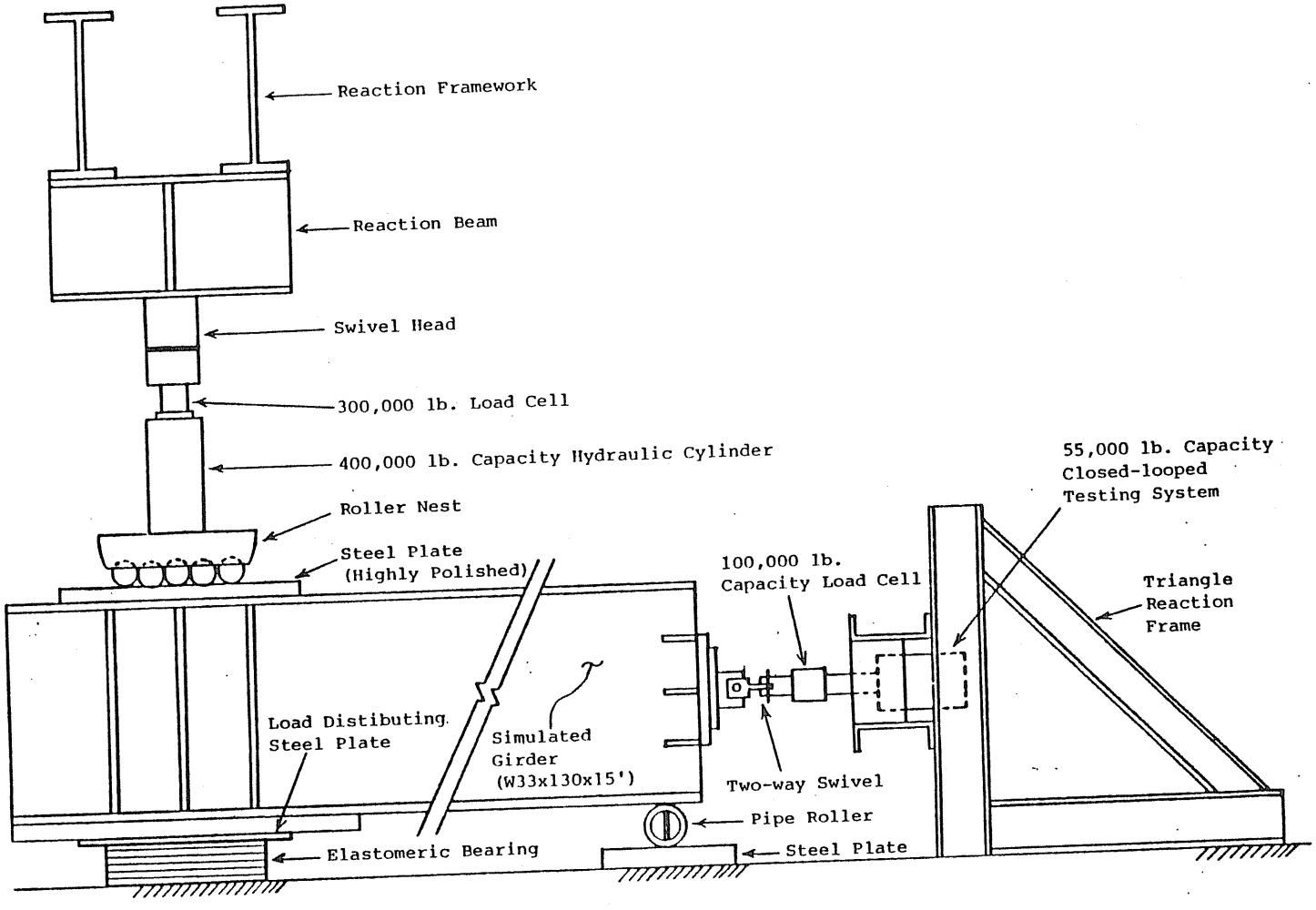

Figure 2.2 Horizontal Load Chain

an analog-to-digital signal converter, and a micro-computer. The applied normal force was measured using a calibrated 300,000 lb. capacity load cell; the horizontal force was measured with a calibrated 100,000 lb. capacity load cell.

The horizontal displacements of the girder and, thus, the top fibers of the elastomeric bearings in the shear stiffness tests were measured using two calibrated wire-type displacement transducers as shown in Figure 2.3. The vertical displacements of the elastomeric bearing in the compressive stiffness tests were measured using the four calibrated LVDT transducers, also shown in Figure 2.3.

The analog signals for the eight instruments were digitized using a 16 channel, differential input, A/D converter with direct interface to a micro-computer. The micro-computer was used to reduce and plot the data in real time. The sample rate was approximately 15 samples per second. In this manner, the instantaneous relationship of the two force and two displacement quantities of the shear stiffness tests, and the force and four displacement quantities of the compressive stiffness tests were determined.

2.3 Testing Procedures

For the shear stiffness tests, each bearing was positioned directly in line with the load chain (the "zero position") and then the normal load was applied. The girder was then pulled, causing the bearing to move to the maximum design shear displacement, pushed back to the "zero position", pushed in the opposite direction to the maximum displacement, and again pulled back to the "zero position". Approximately 1,000 data sets, each set consisting of two force and two displacements readings, were recorded for each shear stiffness test.

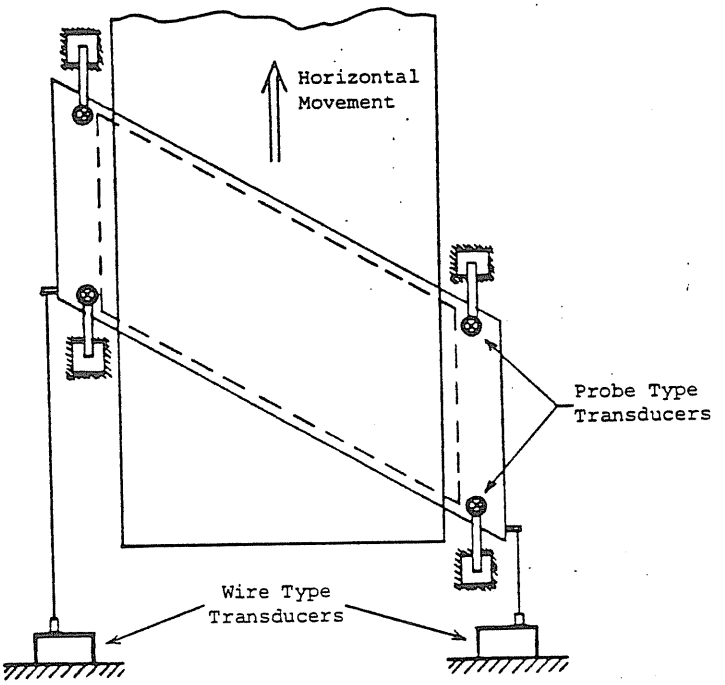

(a) Plan View

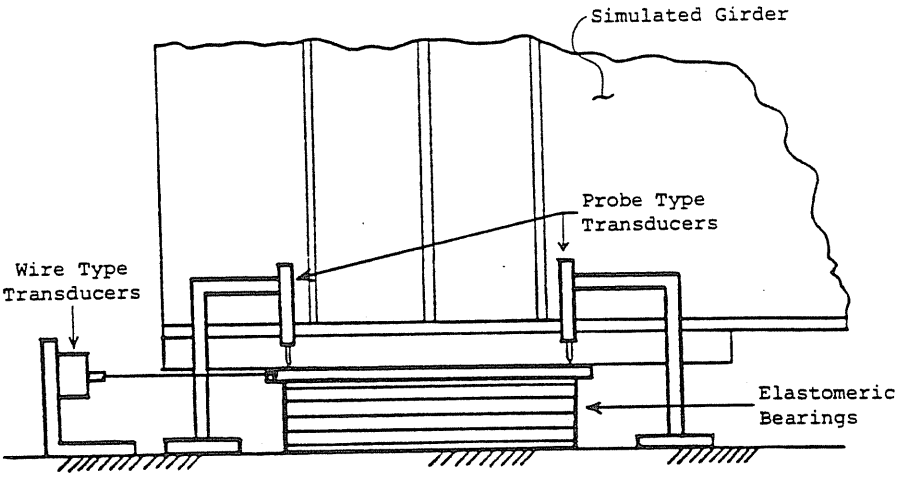

(b) Elevation

Figure 2.3 Instrumentation

The slope of the horizontal force versus horizontal displacement curves is the shear stiffness and was found to be generally linear. For the purpose of this study, it was calculated between the two end points of the curve as shown in Figure 2.4.

Compressive stiffness tests were also conducted for each bearing. The bearings were loaded in increments to the total working load of the bearing. Approximately 500 data sets, each set consisting of a normal load and four displacement readings, were recorded for each test. Since the compressive load versus displacement plots are not linear, an effective compressive stiffness value, k_c, as defined in Figure 2.5 was used to evaluate the fatigue performance of each skewed bearing.

To determine the magnitude of displacements and the number of fatigue cycles to be used in the fatigue testing phase, a rational program had to be formulated. From temperature data for the state of Oklahoma, three sets of temperature ranges, daily, monthly, and yearly, were determined as follows: (1) The average high and low temperatures were first found for Oklahoma City, Oklahoma for each month of the randomly picked years of 1936, 1945, 1962, 1974 and 1981. (2) The average highs and lows for each month were then averaged for the selected years. (3) The daily low-to-high temperature ranges for each day of the month, for all months of the year, were found and averaged so that an average daily range for each month was obtained. (4) The standard deviation of the daily ranges from the monthly average were calculated for each month. This standard deviation was added to the average daily range to obtain a conservative daily range for each month. (5) Steps (3) and (4) were repeated for each of the five years and averaged to obtain the final daily temperature range for

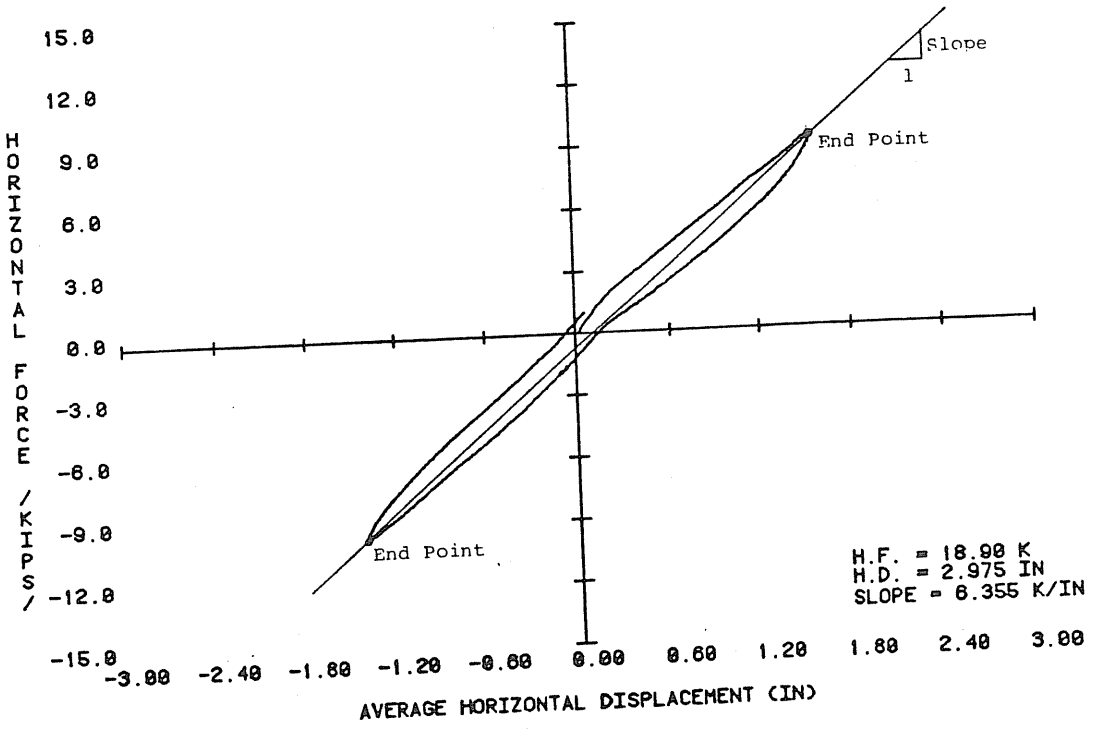

Figure 2.4 Typical Shear verses Displacement Plot

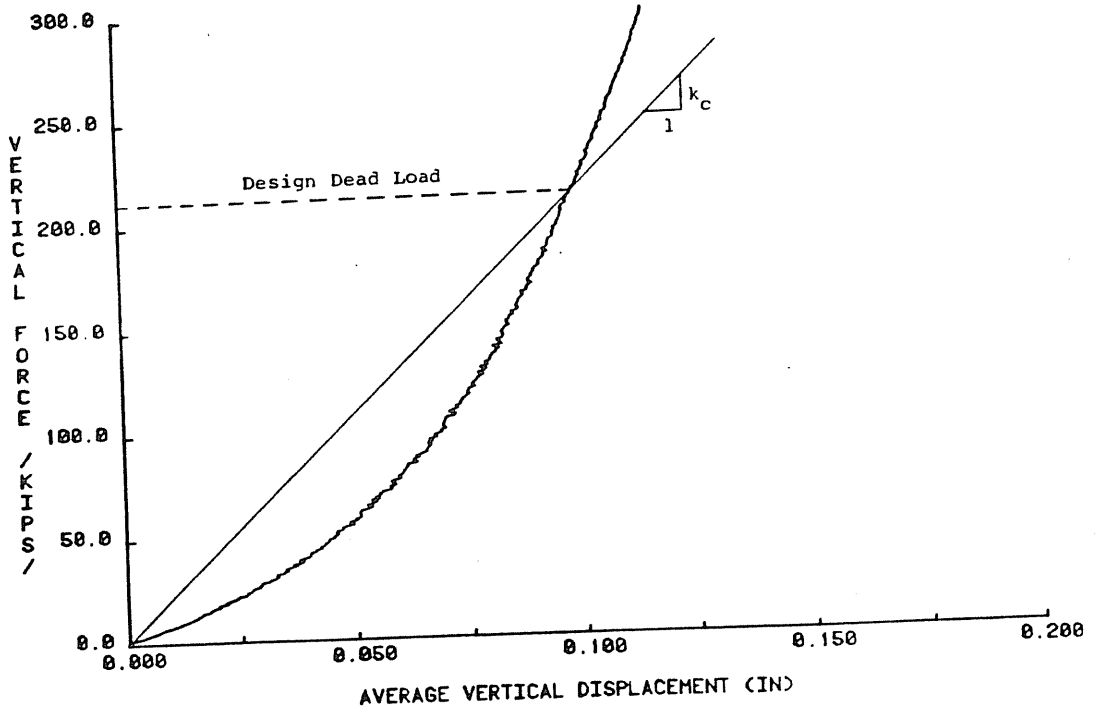

Figure 2.5 Typical Compressive Load verses Displacement Plot

each month of the year. These daily temperature ranges for each month were consistently close to 30°F, so this value was used for each month. (6) The absolute highs and lows for each month were recorded and averaged over the five years to obtain the monthly temperature range for each month of the year. Finally, (7) the absolute highs and lows of the five years were recorded and averaged to obtain the yearly temperature range.

The design life of a bridge built by ODOT is 50 years; therefore, the fatigue program was formulated to simulate the number of environmental cyclic displacements that an elastomeric bearing might be required to deform over a 50 year period. The daily cycles occur 30 times a month for 50 years, or 1500 cycles. The monthly cycle occurs once a month for 50 years, or 600 cycles. The total number of yearly cycles is, of course, 50.

ODOT sets bridge bearings so that there is no shear deformation at a nominal temperature of 60°F. Therefore, 60°F is the zero shear displacement reference point. The temperature ranges for the daily, monthly and yearly cycles with respect to this 60°F reference point are shown in Tables 2.1 and 2.2. With design spans of approximately 200 ft., 300 ft., and 100 ft. for the A, D, and E series bearings, respectively, the coefficient of thermal expansion for steel and the above temperature variations, the corresponding girder displacements were calculated.

For the daily fatigue cycle for a particular month, the girder was first moved from the zero displacement reference point to a displacement corresponding to the average daily temperature for that month (from Step (2) above). The girder was then forced to oscillate around this point a displacement corresponding to a temperature cycle of ±15°F.

Table 2.1

Daily and Monthly Temperature Cycles

Month	Daily Cycles			Monthly Cycles		
	From 60°F move to (°F)	Range (°F)	Number of Cycles	From 60°F move to (°F)	Range (°F)	Number of Cycles
Jan	36.2	±15	1500	39.3	±30.5	50
Feb	41.3	±15	1500	42.0	±34.8	50
Mar	52.6	±15	1500	52.3	±30.3	50
Apr	60.4	±15	1500	58.3	±28.3	50
May	70.5	±15	1500	67.3	±22.1	50
Jun	76.8	±15	1500	76.8	±21.6	50
Jul	83.2	±15	1500	84.7	±19.5	50
Aug	82.1	±15	1500	81.3	±21.9	50
Sep	72.3	±15	1500	70.5	±26.7	50
Oct	63.3	±15	1500	60.1	±25.9	50
Nov	50.3	±15	1500	51.3	±26.7	50
Dec	40.2	±15	1500	40.5	±27.1	50

Table 2.2

Yearly Temperature Cycles

From 60°F move to	Range	Number of Cycles
55.7°F	±48.5°F	50

The monthly and yearly cycles were conducted in a similar manner using the values determined above.

In test Phase IV, each bearing was placed in a deep freeze unit at a nominal temperature of -20°F for approximately 72 hours. Each bearing was taken from the freezer and placed in the test setup as quickly as possible to insure only a small rise in bearing temperature. Immediately upon placement in the test setup and with a compressive force equal to the design dead loading, a shear stiffness test was conducted on the bearing. A temperature probe was embedded in the steel plate of each bearing; plate temperature was measured and recorded at the time of each shear stiffness test in this phase.

CHAPTER III

SUMMARY AND CONCLUSIONS

3.1 Theoretical and Experimental Shear Performance of Elastomeric Bearings

Theoretical Behavior. Contributions to lateral deformations of a bearing other than shear deformations, such as P-Δ effects and lateral bulging of the elastomeric layers, are ignored by the current AASHTO Specifications [1]. AASHTO provisions assume that the shear deformation of a bearing is linearly elastic, e.g. simple shear deformation. The corresponding stiffness, k, is given by

$$k = \frac{G\,A}{T} \tag{3.1}$$

where G = shear modulus, A = plan area of undeformed bearing, and T = sum of the internal elastomeric layer thicknesses, Σt_i.

Although it is often assumed that shape effects can be ignored in simple shear theory, when elastomeric material is subjected to shear forces both shearing and bending occur and the total displacement, Δ_s, is the sum of the displacements due to both effects. Using Southwell's [3] equation for total displacement and taking the modulus of elasticity equal to three times the shear modulus [4], the resulting shear stiffness, including bending effects, is

$$k = \frac{V}{\Delta_s} = \frac{G/T}{(1/A + T^2/36I)} \tag{3.2}$$

where V = shear force and I = the moment of inertia of the bearing plan area taken about an axis perpendicular to the girder axis. The first term in the denominator is the pure shear term; the second term is the pure bending contribution which reduces the horizontal stiffness of the bearing.

Compounding and vulcanization processes required to fabricate reinforced elastomeric bearings effect the properties of the rubber [4]. The most easily measured property of the completed bearing is the "International Degrees of Hardness" measured with a Shore A type durometer. Hardness is then in turn used to define other properties of a completed bearing. Since fabrication processes significantly affect hardness, there is wide scatter in relating hardness to shear modulus. For the purposes of this study, the following ranges of shear moduli were used: 90 to 120 psi for 50 hardness, 120 to 180 psi for 60 hardness, and 180 to 240 psi for 70 hardness [4]. Using the measured hardness (Durometer reading) given in Table 1.2, a value for the theoretical shear modulus was determined for each bearing using the above criteria. With this theoretical shear modulus, the total rubber thickness and the bearing area, the shear stiffness was estimated for each bearing using Equation 3.1 and compared to experimental results.

Experimental Behavior of Skewed Bearings. Experimental results showed that the simple shear equation for estimating the shear stiffness of skewed bearings is very conservative. Further, a direct correlation between predictions and experimental results was not evident. In general, within a bearing pad series, the simple shear predictions of shear stiffness increased as the skew angle decreased from 90° (rectangular) to 30° because of the increase in bearing area.

The experimental shear stiffnesses also increased with decrease in skew angle, but the increase was more rapid than the predicted values. To partially account for the increase in experimental shear stiffness, an effective shear area for each bearing was defined. This effective area was used in conjunction with bending effects to establish a proposed design expression for the prediction of shear stiffness of skewed elastomeric bearings [2]. The proposed shear stiffness expression for any practical skew angle ($\alpha > 0$) is

$$(k_s)_\alpha = \left[\frac{GA/T}{\frac{L}{L - \delta_s} + \frac{(T \sin \alpha)^2}{3[(L \sin \alpha)^2 + (W \cos \alpha)^2]}} \right] \quad (3.3)$$

where δ_s = the maximum required horizontal displacement of the bearing. All other variables are either previously defined (See Nomenclature) or shown in Figure 3.1. This proposed design expression predicts the experimentally determined shear stiffnesses with relatively good correlation as shown in Table 3.1.

Experimental Behavior of Turned Bearings. Five of the original twelve skewed bearings were modified to rectangular bearings after the completion of the six test phases described in Section 1.4. These modified bearings were tested in various "turned" positions to determine the effects of orientation on shear stiffness.

Using an effective area coupled with bending effects, similar to that used for the development of the skewed bearing prediction expression, a proposed design expression for the prediction of shear stiffness for rectangular bearings with turned shear axes was developed [2]:

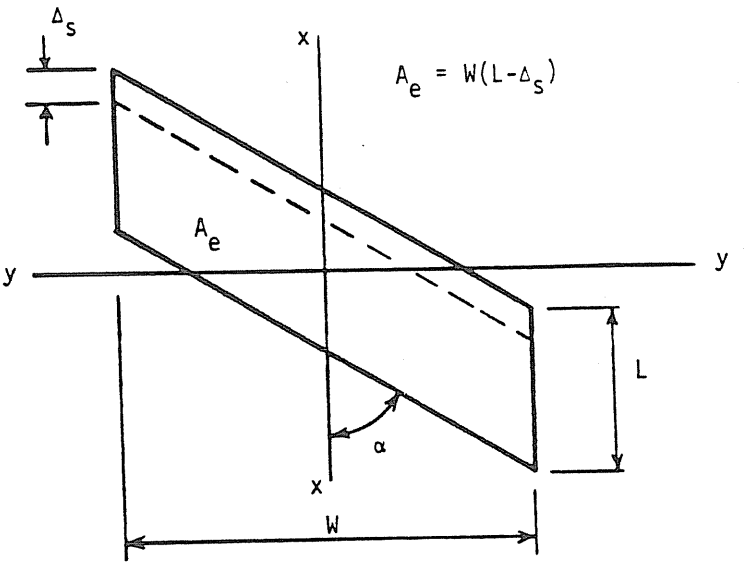

Figure 3.1 Skewed Bearing Parameters

Table 3.1

Comparison of the Experimental and Proposed Prediction Equation Results for Skewed Bearings

Bearing	Shear Stiffness (kips/in)		Ratio: Predicted to Measured
	Measured	Predicted	
A90	3.62	4.58	1.27
A60	6.36	6.16	0.97
A45	5.63	5.96	1.05
A30	7.31	7.17	0.98
D90	3.68	4.20	1.14
D60	5.22	5.45	1.04
D45	5.46	5.59	0.98
D30	6.77	6.36	0.94
E90	16.91	20.42	1.21
E60	20.50	24.51	1.20
E45	18.26	22.98	1.26
E30	24.69	27.69	1.12
A45-M90	3.49	3.83	1.10
A60-M90	4.37	4.64	1.06
A30-M60	3.96	4.50	1.14
A30-M45	5.16	5.67	1.10
A30-M90A	2.99	3.42	1.14
A30-M90B	2.05	2.25	1.10

Note: All measured shear stiffness values were determined after the six test phases.

$$(k_t)_\alpha = GA/T \left[\frac{\sin^2\alpha}{\frac{b}{b - \delta_s} + \frac{T^2}{3b^2}} + \frac{\cos^2\alpha}{\frac{a}{a - \delta_s} + \frac{T^2}{3a^2}} \right] \quad (3.4)$$

All variables are either previously defined (See Nomenclature) or shown in Figure 3.2. Again, relatively good correlation between predicted and experimental results was found as shown in Table 3.2.

It should be noted that both Equations 3.3 and 3.4 reduce to the same expression for rectangular bearings that are orientated perpendicular to the bridge girder axis.

3.2 Shear Behavior of Elastomeric Bearings Subjected to Low Temperatures

The effects of temperature on the shear modulus of rubber are best described as a thermal stiffening at lower temperatures. Low temperatures induce a phenomenon called crystallization which locks the elastomer fibers together resulting in a much stiffer material. Table 3.3 shows the shear modulus ratio of low-to-normal temperatures, as published by Minor and Egen [5]. The effect of low temperatures on the shear modulus is not linear and the rate of crystallization is most rapid at approximately 10°F.

In the low temperature tests of Phase IV, the average recorded bearing temperature at the time of testing was 3.7°F. The average increases in shear stiffness between Phases IV and III for bearing types "A", "D", and "E" were 39%, 45% and 27%, respectively. These percent increases in shear stiffness are well within design values shown in Table 3.3 for rectangular, unturned bearings. Hence, the proposed shear stiffness prediction equations need only be corrected using published values to account for the increase in shear stiffness of elastomeric bearings when at low temperatures.

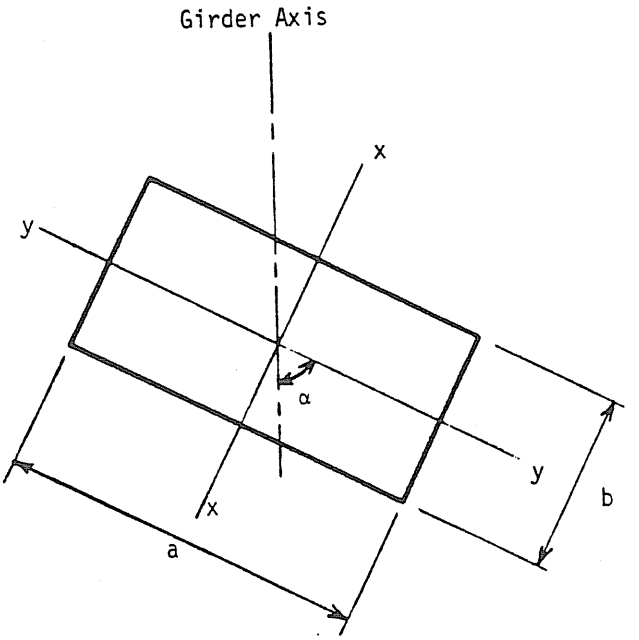

Figure 3.2 Turned Bearing Parameters

Table 3.2

Comparison of the Experimental and Proposed Prediction Equation Results for Turned Bearings

Bearing	Alpha (deg) (Tα)	Shear Stiffness (kips/in)		Ratio: Predicted to Measured	Ratio Normalized to T90
		Measured	Predicted		
A30-M90A	T90	2.99	3.42	1.14	1.00
	T60	3.28	3.64	1.11	0.97
	T45	3.42	3.86	1.13	0.99
	T30	3.56	4.07	1.14	1.00
	T00	3.77	4.29	1.14	1.00
A30-M90B	T90	2.05	2.25	1.10	1.00
	T60	2.13	2.36	1.11	1.01
	T45	2.24	2.46	1.10	1.00
	T30	2.36	2.57	1.09	0.99
	T00	2.44	2.67	1.09	0.99
A45-M90	T90	3.49	3.83	1.10	1.00
	T60	3.57	4.01	1.12	1.02
	T45	3.65	4.19	1.15	1.05
	T30	3.97	4.36	1.10	1.00
	T00	4.14	4.54	1.10	1.00
A60-M90	T90	4.37	4.64	1.06	1.00
	T60	4.47	4.78	1.07	1.01
	T45	4.59	4.91	1.07	1.01
	T30	4.72	5.04	1.07	1.01
	T00	4.59	5.17	1.13	1.07
A90	T90	3.48	4.58	1.32	1.00
	T60	3.70	4.73	1.28	0.97
	T45	3.75	4.87	1.30	0.98
	T30	3.88	5.01	1.29	0.98
	T00	3.94	5.15	1.31	0.99

Note: All measured shear stiffness values were determined after the six test phases were conducted.

Table 3.3

Shear Modulus Ratio For Low-to-Normal Temperatures
(From Reference 5)

Durometer Reading (Hardness)	Ratio for Temperatures Of:				
	40°F	20°F	0°F	-20°F	-40°F
50	1.00	1.00	1.10	1.25	1.55
60	1.05	1.25	1.65	1.90	2.05
70	1.05	1.15	1.50	1.85	2.15

3.3 Fatigue Performance of Skewed Bearings

Shear Stiffness Degradation. Shear stiffness tests were conducted before and after the bearings were subjected to the fatigue programs of Phase II (horizontal surfaces) and Phase V (2% sloped surfaces). In general, fatigue cycles applied with parallel bearing contact surfaces did not significantly affect the post-fatigue shear stiffness of the bearings; the average deterioration was 1.2%.

For the second series of fatigue tests, the bearings were rotated to a 2% slope with respect to the simulated bridge girder horizontal centerline. The values of shear stiffness after "rotated fatigue" decreased by an average of 8.2% when compared to the post-parallel fatigue values.

The effects of fatigue on skewed bearings with a girder end rotation are slightly larger than those for bearings with parallel bearing surfaces. However, after a total of 100 years of simulated environmental induced shear displacements, the degradation of shear stiffness was not substantial.

Compressive Stiffness Degradation. Compressive stiffness tests were also conducted before and after the shear fatigue program of Phase II. Since the compressive load versus displacement plots are not linear, an effective compressive stiffness value, k_c, as defined in Section 2.3 and Figure 2.5, was used to evaluate the fatigue performance of each skewed bearing.

For all but three bearings, the compressive stiffness values determined in Phase III were slightly greater (attributed to the method of evaluation) than the values determined in Phase I. Thus, it is concluded that the shear fatigue does not significantly effect the compressive stiffness of skewed elastomeric bearings.

REFERENCES

1. American Association of State Highway and Transportation Officials, "Standard Specifications for Highway Bridges:, 13th Edition, 1985 Interim Section 14", Washington D.C., 1985.

2. Allen, G.D. and T.M. Murray, "Experimental Investigation of Skewed Elastomeric Expansion Bridge Bearings", Final Report FSEL/ODOT 86-01 submitted to the Oklahoma Department of Transportation, Fears Structural Engineering Laboratory, University of Oklahoma, August 1986, 130 pages.

3. Southwell, R.V., Introduction to the Theory of Elasticity, 2nd Edition, Oxford University Press, 1944.

4. Stanton, J.F., and C.W. Roeder, "Elastomeric Bearing Design, Construction, and Materials", Transportation Research Board, NCHRP Report No. 248, Washington D.C., 1982.

5. Minor, J.C., and R.A. Egen, "Elastomeric Bearings Research", Transportation Research Board, NCHRP Report No. 109, Washington, D.C., 1970.